Four-Regime Speed–Flow Relationships for Work Zones with Police Patrol and Automated Speed Enforcement

K. A. Avrenli, Rahim F. Benekohal, and Hani Ramezani

This paper presents the development of a four-regime speed–flow relationship for highway work zones and the effects of police presence (police) and speed photo enforcement (SPE) on the speed–flow relationship and capacity. The base data were collected when signage typical of that shown in the *Manual on Uniform Traffic Control Devices* for an Interstate highway work zone with no lane reduction was present. Police and SPE data were collected, respectively, when a police patrol car and an SPE van were added to the typical work zone. From each data set, the step-by-step progression from a three-regime model based on least-squares regression to a four-regime speed–flow curve is presented. The four-regime model comprises four equations: (*a*) horizontal line for free-flow regime that covered the volume levels up to 900 passenger cars per hour per lane, (*b*) fourth-degree spline for the upper transition part of the speed–flow curve, (*c*) another fourth-degree spline for the lower transitions part, and (*d*) equation in the form of power function for the highly congested part of the speed–flow relationship. The speed–flow curve for the base case had a free-flow speed (FFS) of 61.3 mph and a capacity of 1,850 per car per hour per lane (pcphpl). In the police case, however, the FFS and capacity were reduced by 6.3 mph and 50 pcphpl, respectively. For the SPE case, the FFS and capacity were also reduced by 6.8 mph and 100 pcphpl, respectively. The new curves provided the more accurate speed and work zone capacity estimations required for efficient operation.

Some work zones may create congestion bottlenecks on roadway systems. Nonrecurring conditions, such as inclement weather and traffic incidents, account for approximately 50% of all U.S. highway congestion. Work zones cause about 24% of nonrecurring delays on freeways (*1*). The loss of capacity caused by work zones was estimated to be 60 million vehicles per hour per day over a 2-week period when the summer roadwork season was at its peak in 2001 (*2*). In addition to congestion, safety in work zones may be of concern. In 2009, motor vehicle crashes in U.S. work zones led to 667 fatalities (*3*). In terms of dollars, highway work zone fatalities cost at least four times more than total U.S. construction (*4*). Rear-end collisions in general were the most predominant type of crash in work zones, a finding attributable to high-speed variation among vehicles and excessive vehicle speed (*5, 6*). Thus speed control strategies, such as police presence (police) and intelligent transportation systems (ITS), such as speed photo enforcement (SPE), have been implemented in work zones. Although several studies (*7–12*) have explored the speed-reduction effects of police and ITS in work zones, their effects on the relationship of work zone speed and capacity have not been examined extensively. Only a limited number of studies have analyzed the speed–flow relationship of work zones when police or an ITS was implemented in work zones.

The objectives of this study were to

- Establish multiple-regime speed–flow curves from field data to represent the speed–flow relationship for a selected work zone during police and SPE implementation,
- Assess how the speed–flow relationships during police and SPE implementation compared with the speed–flow curve of the same work zone without them (i.e., base conditions), and
- Determine the impacts of police and SPE on work zone capacity compared with base conditions.

Field data from work zones were collected and speed–flow curves were developed. From each data set, the progression is presented from a three-regime model, on the basis of least-squares regression, to a four-regime speed–flow curve with free-flow speed (FFS), volume, and capacity constraints.

BACKGROUND

Work zone capacity is not explicitly defined in *Highway Capacity Manual* 2000 (*13*). The following definitions were used in the literature to define work zone capacity:

- "The discharge flow when there is a continuous flow of traffic" (*14*),
- "The traffic flow rate just before a sharp speed drop followed by a sustained period of low vehicle speed and fluctuating traffic flow rate" (*15*),
- "The mean queue discharge flow rate from the bottleneck that was located at the end of the transition area" (*16*),
- "95th percentile value of all 5-min within-a-queue flow rate" (*17*), and
- "The average volume of the ten highest volumes immediately before and after queuing conditions" (*18*).

Several studies have developed relationships between work zone capacity and other factors. Al-Kaisy et al. identified significant

K. A. Avrenli and H. Ramezani, Room B106, and R. F. Benekohal, Room 1213, Newmark Civil Engineering Laboratory, Department of Civil and Environmental Engineering, University of Illinois at Urbana–Champaign, Urbana, IL 61801. Corresponding author: K. A. Avrenli, avrenli2@illinois.edu.

Transportation Research Record: Journal of the Transportation Research Board, No. 2272, Transportation Research Board of the National Academies, Washington, D.C., 2012, pp. 35–43.
DOI: 10.3141/2272-05

effects of temporal variation related to driver characteristics, grade, day of week, and weather conditions on work zone capacity (*16*). Kim et al. developed a linear regression model to estimate capacity for short-term work zones (*19*). Karim and Adeli proposed a radial basis function neural network model to estimate work zone capacity (*20*). Adeli and Jiang developed a neuro-fuzzy logic model to estimate work zone capacity (*21*). Benekohal et al. developed a step-by-step methodology to estimate the operating speed and capacity in work zones (*22*). Racha et al. investigated traffic behavior in work zones for planning purposes (*23*).

Only a few studies have examined the effects of ITS on work zone capacity. Kang, Chang, and Zou proposed a variable speed limit system that could increase the work zone throughput by up to 20% and reduce the average delay per vehicle by up to 34% (*24*). Kang, Chang, and Panacha found that dynamic late merge could lead to up to an 11% increase in work zone throughput compared with no-merge control (*25*). Yulong and Leilei developed an intelligent lane merge control system similar to dynamic late merge (*26*). According to the results of their study, dynamic late merge control and intelligent lane merge increased the work zone capacity by 8% and 20%, respectively, compared with static late-merge control. None of these studies explored the effects of police and SPE on the work zone speed–flow relationship.

DATA COLLECTION AND REDUCTION

To capture the distinct effects of police and SPE on work zone speed–flow relationship in cases in which demand is under or near capacity conditions, three data sets were collected in a work zone located on I-55 northbound at Milepost 259, near Chicago, Illinois. The work zone had no lane closures, and two lanes were open in each direction of traffic. The work activity area was separated from the open lanes by concrete barriers. The work included construction of an additional lane and bridge deck repair. The length of the work zone was about 7 mi. The posted speed limit in the work zone was 55 mph, whereas it was 65 mph outside of the work zone. All three data sets were collected during afternoon, off-peak hours in June 2007. To avoid the effects of volume variation, all three data sets were collected on weekdays and at similar times of day. No data were collected during peak hours, because downstream congestion could have reached the data collection location. Because such congestion did not stem from police and SPE implementations, the resulting data could not reflect the effects of the speed reduction treatment accurately.

Data were collected for the following conditions:

1. Base. Typical signage cited in the *Manual on Uniform Traffic Control Devices* was in place.
2. Police. In addition to the presence of standard manual signage, a police patrol car was parked on the right shoulder. The police patrol car did not have its lights on, and the police officer stayed inside the car. However, the patrol car was clearly visible to approaching drivers in the work zone. The 7-mi work zone started at Milepost 255, and the police patrol car was located at Milepost 259.
3. SPE. In addition to the presence of standard manual signage, an SPE van was parked on the right shoulder. The SPE van was parked partially on paved shoulder and partially on gravel shoulder, and a sign that displayed the speeds of approaching vehicles was displayed on the roof of the van. Drivers were able to clearly see that the SPE van was present and that the speed display sign showed their speed. The SPE van was located at the same milepost at which the police car was parked.

The data were collected for several hours for each treatment. Because of the extensive time required for data reduction, however, only approximately 1 h of traffic flow data was used from each data set. The number of vehicles analyzed in each data set was more than 2,000. To obtain information on individual vehicles, the traffic flow data were collected by a video camera. The video camera was situated at the site such that it did not interfere with the work zone traffic flow. The camera captured vehicles as they passed two markers placed about 200 ft apart from each other near the shoulder. The markers were situated several hundred feet downstream of the treatment location (i.e., either the police car or the SPE van). Thus motorists had sufficient time to respond to the treatment and reduce their speeds before they were captured on the video camera. All vehicles that changed lanes between the two markers were excluded from the data. In each data set, the number of vehicles that changed lanes between the two markers was less than 0.5% of the total number of vehicles observed.

Time stamps and frame numbers in the video files provided a reading of a particular frame within 1/30th of a second, which resulted in the accuracy of 1 mph for speed computations. The following data were obtained for each vehicle from the video files in all three data sets:

1. Vehicle type classified into one of two categories:
   – Passenger car: cars, pickup trucks, sport utility vehicles, and minivans and
   – Heavy vehicle: single-unit trucks, semitrailers, combination trucks, and buses.
2. Vehicle lane of travel:
   – Median lane and
   – Shoulder lane.
3. Times at which vehicle passed the two markers.

To compute the speed of a particular vehicle, the observed travel distance between the two markers was divided by the corresponding travel time. Vehicle headways were computed through the use of the times at which successive vehicles passed one of the selected markers.

Preliminary data analyses showed that the presence of the treatments significantly reduced the mean speed of traffic. The mean speeds were 58.4, 53.1, and 51.4 mph for the base, police, and SPE data, respectively. The mean flow rates were 1,321, 1,239, and 1,301 per car per hour per lane (pcphpl) for the base, police, and SPE data, respectively. Because mean flow rates were close to each other and because other affecting conditions were similar, such as weather condition and data collection time, the speed reduction could be attributed to the presence of the treatments. As a result, this paper developed speed–flow curves by which to estimate the effect of the treatments on capacity and on operating speed.

To develop speed–flow curves, data from all traffic conditions were needed while at the site at which the three data sets were collected. Demand did not exceed capacity, and no queue formed as a result of excessive demand. Thus, for overcapacity conditions, data were used that had been collected from I-55 and I-74, where traffic in a single lane of the highway exceeded the capacity of the roadway. Data were collected and reduced in a way similar to the procedure mentioned above. When demand exceeded the capacity and a queue developed, speed–flow characteristics in the congested segment of a one-lane section were similar to the corresponding segment on a

two-lane segment. For oversaturated conditions, use of the speed–flow curve from the one-lane segment (although not ideal) was a reasonable approach when the two-lane segment did not become oversaturated, and the data for the highly congested condition could not be collected at the site. This issue is discussed in the subsection on the congestion regime.

ANALYSIS AND RESULTS

Three-Regime Speed–Flow Curves

Many resources establish (e.g., in *Highway Capacity Manual,* 2000) that, for low to moderate flow conditions on multilane highways, speed remains constant as flow increases. This part of the speed–flow curve represents the free-flow regime and is in the form of a horizontal line. Beyond this volume level, the speed decreases as the flow increases up to the capacity level (transition regime for the speed–flow curve). Any further decrease in speed (from the speed at capacity) also decreases flow until flow and speed both reach a value of zero (congested regime).

Avrenli et al. developed three-regime work zone speed–flow curves with the scatter data shown in Figure 1 (*27, 28*). The data from each data set were aggregated over 2-min intervals. An interval length of 2 min was selected to aggregate the speed–flow data because Avrenli et al. showed that interval lengths shorter than 2 min might indicate too much fluctuation in speed or flow rate (*27*). Interval lengths greater than 2 min (e.g., 15 min) might obscure some of the fluctuations in speed and flow, and might lead to too much averaging of the data.

In this study, the upper (uncongested) branch of the three-regime speed–flow curves was revised. Then some problems with these curves were addressed. To eliminate the problems, four-regime speed–flow curves were built on the basis of the revised curves. The subsections that follow offer details about the three-regime speed–flow curves.

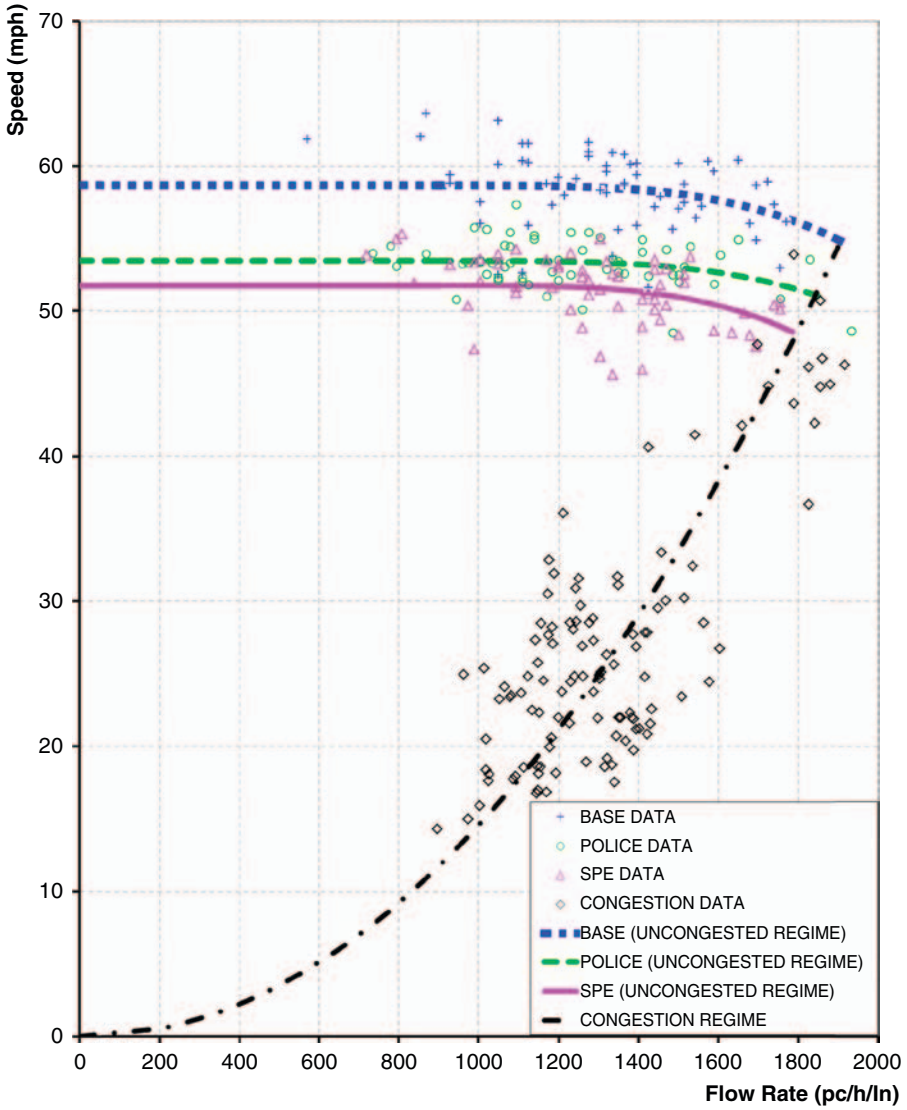

FIGURE 1 Three-regime speed–flow curves for base, police, and SPE data (see also Figure 3*a*; pc/h/ln = passenger cars per hour per lane).

Free-Flow Regime

Avrenli et al. set the upper threshold for the free flow to about 800 pcphpl and found that the speed–flow relationship was a horizontal line at the FFS for this region. (*27, 28*). In the research reported in this paper, a free-flow threshold of 900 pcphpl was used. The 900 corresponded to a 4.0-s headway used as one of the criteria to distinguish in-platoon vehicles from free-flowing vehicles. This study used the same platooning criteria as Benekohal et al. (*14*). A vehicle was considered to be in free-flow condition if it maintained a time headway of 4.0 s, or greater, and a space headway of 250 ft or greater. The FFSs were estimated from the regression of the noncongestion data shown in Figure 1. They are explained in the following subsection.

Transition Regime

During the transition regime, average speeds started to decrease with the increasing flow rate, but no flow breakdown occurred. The transition regime extended from the end of the free-flow regime (i.e., for flow rates of 900 pcphpl or greater) to the point of maximum flow rate, which determined work zone capacity. The transition regime was found from the least-squares estimation of the noncongestion data shown in Figure 1. For the base, police, and SPE data sets, all data points that had a flow rate of 900 pcphpl or greater were used in the regression. On the basis of the nonlinear regression, the transition regime was represented by Equation 1, *a*, *b*, and *c* for the base, police, and SPE data, respectively.

$$U = \text{FFS} - (\text{FFS} - 18.7) * \left(\frac{Q - 900}{2{,}182.2 - 4.3 * \text{FFS}} \right)^{3.6} \quad (1a)$$

$$U = \text{FFS} - (1.0 * \text{FFS} - 19.6) * \left(\frac{Q - 900}{2{,}195.5 - 4.1 * \text{FFS}} \right)^{3.6} \quad (1b)$$

$$U = \text{FFS} - (1.1 * \text{FFS} - 13.4) * \left(\frac{Q - 900}{2{,}105.9 - 5.5 * \text{FFS}} \right)^{3.6} \quad (1c)$$

where

U = average speed (mph), $U_{optimum} \le U <$ FFS;
$U_{optimum}$ = speed at maximum flow rate (i.e., Q_{max});
Q = flow rate (pcphpl), $900 < Q \le Q_{max}$; and
FFS = 58.7, 53.5, and 51.8 mph through nonlinear regression of base, police, and SPE data, respectively.

The format of Equation 1*a, b,* and *c* was similar to that suggested by the 2000 *Highway Capacity Manual* for basic freeway sections (*13*).

Congestion Regime

The congestion regime represented traffic conditions in which demand exceeded the work zone capacity. The research team did not observe traffic congestion in base, police, or SPE cases. It was assumed that congested speed–flow relationships would be similar for the base, police, and SPE cases. Although this assumption was reasonable, to verify it on the basis of filed data in which SPE and police caused the congestion was practically impossible. Police or SPE usually are used in uncongested conditions to increase speed limit compliance. If either of them happened to be in a congested work zone, chances are it was not they that caused the congestion.

To develop a speed–flow relationship for the congestion regime, data were used from two comparable Interstate highway work zones with congested conditions. The congested data were suitable for this analysis because one of the work zones was on the same Interstate highway and the other was a similar rural Interstate highway. The data used for the congested part came from I-74 eastbound at Milepost 5 and from I-55 northbound at Milepost 55. Both sites had a posted speed limit of 55 mph and similar work intensities during the data collection. Although the sites where the congestion data were collected had one lane open within the work activity area, it was assumed that whether one lane was open, or two, did not significantly alter the speed–flow relationship in congested conditions because there was practically no opportunity to pass (*27,28*).

The congestion regime of the work zone speed–flow curve is represented by Equation 2, which is a power function built from least-squares estimation of the congestion data.

$$Q = 271.43 * U^{0.4868} \quad (2)$$

The models developed thus far are the free-flow regime, transition regime, and congestion regime. Their combination results in a three–regime model. Some problems with the three-regime models are discussed in the following section.

Problems with Three-Regime Speed–Flow Curves

Avrenli et al. pointed out the following issues with the three-regime speed–flow curves and recommended improvements (*27, 28*):

- As shown in Figure 1, sharp transitions occurred between the upper (uncongested) and lower (congested) branches of the speed–flow curves for the base, police, and SPE data. The sharp transitions occurred at the point of maximum flow (i.e., work zone capacity) because the first derivatives of the transition and congestion regimes did not match at that point. Thus the speed–flow curves shown in Figure 1 might not depict accurately the speed–flow relationship close to capacity conditions.
- For each data set, the point of maximum flow (i.e., capacity) was found from the intersection of two curves (i.e., congestion regime and transition regime). However, the work zone capacity should have been estimated instead from more detailed analysis of each data set and the characteristics of platooning vehicles.

Thus there is a need to improve the three-regime model. To provide a more accurate representation of the traffic conditions observed in the work zone, four-regime speed–flow curves were developed for the base, police, and SPE scenarios. These curves are described in the section that follows.

Four-Regime Speed–Flow Curves

Free-Flow Regime

To explore the relationship between speed and flow for the free-flow regime, it is necessary to be careful in the aggregation of the data so that the traffic flow in the interval is uniform. This effort requires a large number of data points for low volume conditions. When

such data points are not available, the relationship may be observed between speed and instantaneous flow rate of individual free-flowing vehicles to examine the speed–flow relationship for the free-flow regime. Figure 2, *a*, *b*, and *c*, shows the scatterplot of speed versus instantaneous flow for the free-flowing vehicles in the base, police, and SPE data, respectively. A least-squares linear model was fit to each data set. However, the slopes of these lines were not significantly different from zero at $\alpha = 0.05$, because the *p*-values for the slope were .28, .40, and .77 for the base, police, and SPE scenarios, respectively. The average speed of the free-flowing vehicles, with the exclusion of the platoon leaders, was used as the vertical intercept for the horizontal line. This approach led to 61.3, 55.0, and 54.5 mph for the base, police, and SPE data, respectively.

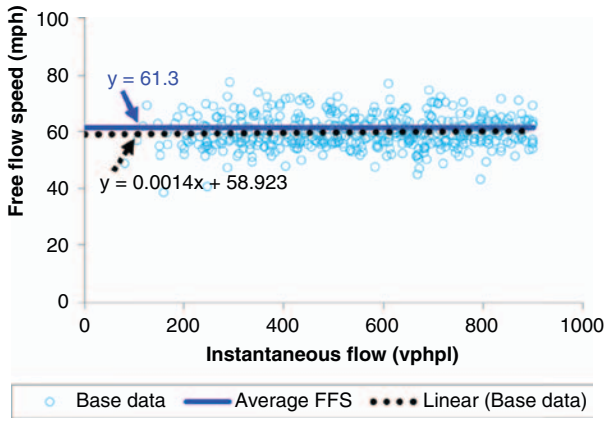

(a)

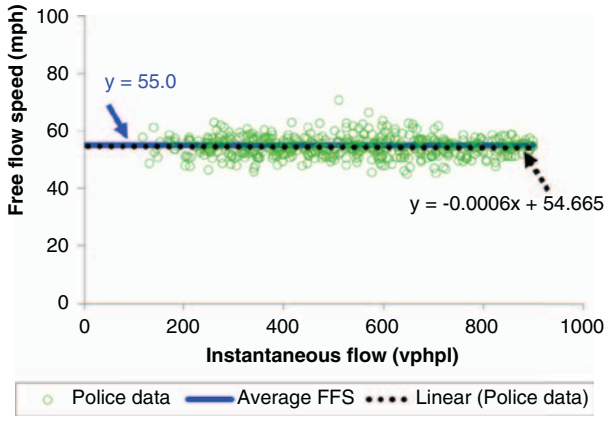

(b)

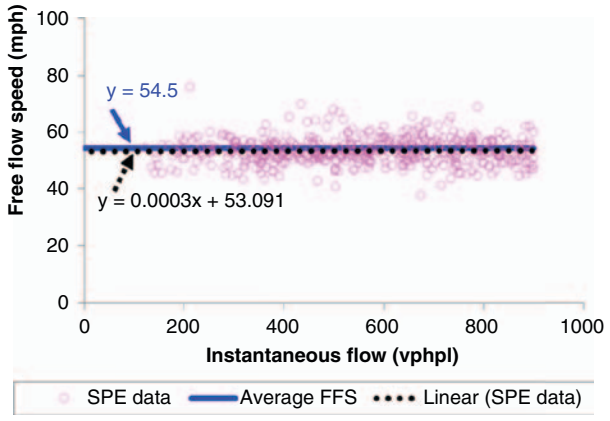

(c)

FIGURE 2 Speed versus instantaneous flow of free-flowing vehicles for (*a*) base, (*b*) police, and (*c*) SPE data (vphpl = vehicles per hour per lane).

Upper Transition Regime

Figure 3*a* shows the general form of the three-regime speed–flow curves, and 3*b* shows the general form of the four-regime speed–flow curves. The four-regime models have upper and lower transition regimes instead of a single transition regime to provide piecewise smooth transition between the upper and lower branches of the speed flow curves. Similar to the free-flow regime, the upper transition regime represents traffic conditions with no flow breakdown. The upper transition regime is the part of the speed–flow curve between the end of the free-flow regime and the point of maximum flow.

For the base, police, and SPE data, the point with the maximum flow rate was determined with the same methodology proposed by Ramezani et al. (*29*), except the calculations were performed for every minute of the data instead of the entire study period. A lower bound for capacity (Table 1, Column 2) was computed from the h-n method as suggested by Ramezani et al. (*29*). A higher bound, called the "potential capacity," was computed from the average headway of the vehicles (except for the leader of platoons) in platoons with more than four vehicles. The moving average flow rates for 15-min data by 1 min increments were then computed, and the maximum 15-min flow rate was obtained for each data set. The unrounded capacity was computed as the product of the potential capacity and platooning factor. The platooning factor was estimated through a consideration of how close the lower bound and the upper bound were to each other, as well as traffic conditions (i.e., whether or not queuing occurred after traffic breakdowns). In these data sets, there was no after-breakdown queuing, so the platooning factor was computed through the division of the lower bound (Table 1, Column 2) by the 95% of the upper bound value (Table 1, Column 3). To find work zone capacity, the unrounded capacity was rounded to the nearest 50 pcphpl (Table 1, Column 6). The h-n method may not give reasonable results if the proportion of vehicles that maintain headways close to the value of h is high. When this happens, the platooning factor will be considerably lower than about 0.70.

To compute the optimal speed, the speed that corresponds to the capacity (Table 1, Column 6) was found from Equation 1, *a*, *b*, and *c*, for the base, police, and SPE data, respectively. For each case, the speed that corresponded to the capacity was found from Equation 2. For each case, the optimal speed was determined as the average of those found from Equations 1 and 2 (Table 1, Column 9). This optimal speed calculation was different from the one suggested by Ramezani et al. (*29*) because it was more suitable for conditions in which not enough field data were at capacity, which was the case here. At this study site, no lane was closed or dropped, so the chance that close-to-capacity conditions would be observed was lower than in a work zone with lane closure. The number of data points close to capacity conditions was low for each data set. For this reason, this new method to find the optimal speed was applied.

Once the capacity and optimum speed were estimated, the speed–flow curve had to go through that point. Polynomial functions of

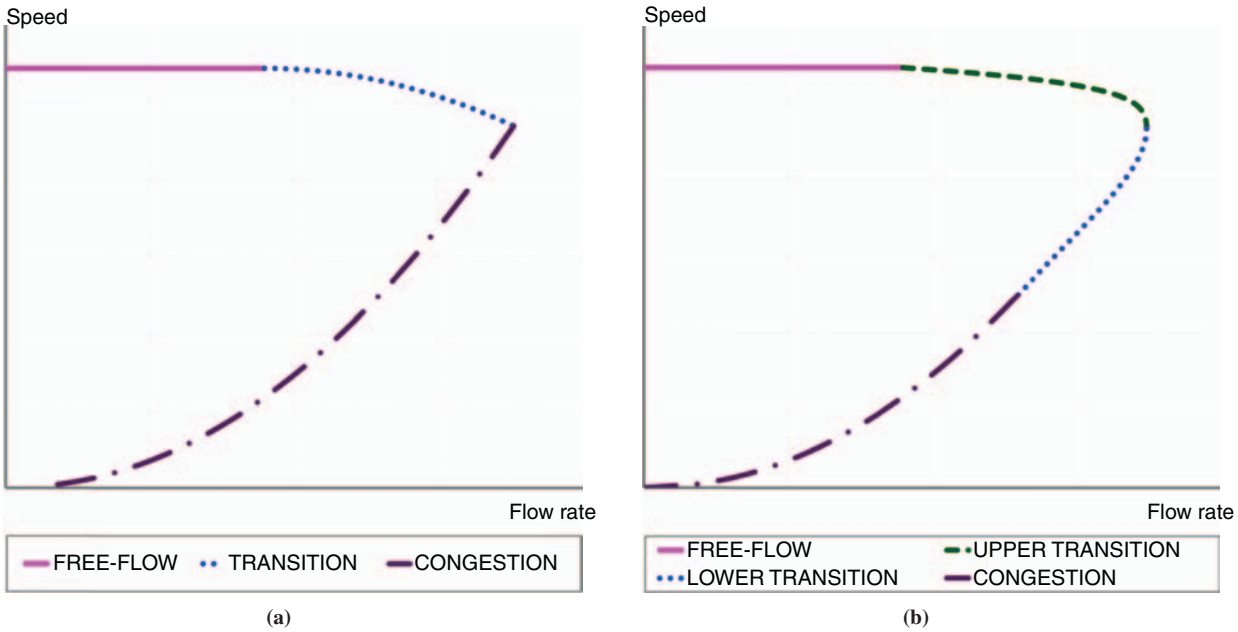

FIGURE 3 General form of (*a*) three-regime speed–flow curves and (*b*) four-regime speed–flow curves.

degree 4 were used for the upper and lower transition regimes. Equation 3 shows the general form of these functions.

$$Q = a * U^4 + b * U^3 + c * U^2 + d * U + e \quad (3)$$

where a, b, c, d, and e are coefficients of the polynomial function.

The coefficients of the upper transition model in Equation 3 were determined through the fitting of a fourth-degree spline between the end of the free-flow regime and the point with the maximum flow rate. Equation 4a, b, and c represents the upper transition regime for the base, police, and SPE, respectively.

$$Q = -0.1021695 * U^4 + 20.882107 * U^3 - 1{,}598.66783 * U^2 + 54{,}328.7380 * U - 689{,}614.193 \quad (4a)$$

$$Q = 1.0499253 * U^4 - 222.084320 * U^3 + 17{,}562.01613 * U^2 - 615{,}531.8800 * U + 8{,}071{,}860.334 \quad (4b)$$

$$Q = -0.1615912 * U^4 + 29.738536 * U^3 - 2{,}052.75082 * U^2 + 62{,}989.8415 * U - 723{,}276.525 \quad (4c)$$

Lower Transition Regime

The lower transition regime started at the point of the maximum flow rate (and optimal speed), and connected to the congestion regime at a flow rate of 1,300 pcphpl. The latter flow rate was chosen to maintain a smooth transition to the congested regime model and to keep the overall shape of the lower branch of the speed–flow curves as close as possible to Equation 2, which was obtained from the field data for congested conditions.

The coefficients of the lower transition model were determined by fitting a fourth-degree spline between the point of work zone capacity and a point on the congestion regime at which flow was 1,300 pcphpl. Given the points at which two adjacent regimes connected to one another, the coefficients were calculated such that the functions of the two adjacent regimes had equal value: equal first derivative and equal second derivative at the connection point. In addition, the first derivative of the upper and lower transition regimes was set to zero at the point with the maximum flow rate. Equation 5, a, b, and c, represents the lower transition regime for the base, police, and SPE, respectively.

$$Q = -0.0003204 * U^4 + 0.033693 * U^3 - 1.32543 * U^2 + 48.4619 * U + 516.233 \quad (5a)$$

TABLE 1 Summary of Work Zone Capacity Calculations

Data Set	Maximum Flow Rate from h-n Method (C_h) (pcphpl)	Maximum Flow Rate from Platooning Vehicles (C_p) (pcphpl)	Platooning Factor (PF) $\left(\frac{C_h}{C_p * 0.95}\right)$	Work Zone Capacity (PF$*C_p$)	Work Zone Capacity Rounded to Nearest 50 (pcphpl)	Speed at Capacity from Equation 1 (C_1) (mph)	Speed at Capacity from Equation 2 (C_2) (mph)	Optimal Speed $\left(\frac{C_1 + C_2}{2}\right)$ (mph)
Base	1,748	2,403	0.77	1,840	1,850	55.2	51.6	53.4
Police	1,689	2,459	0.72	1,777	1,800	51.3	48.7	50.0
SPE	1,665	2,318	0.76	1,753	1,750	48.6	46.0	47.3
SPE (unused 2nd h of data)	1,671	2,432	0.72	1,759	1,750	48.6	46.0	47.3

$$Q = -0.0005902 * U^4 + 0.065160 * U^3 - 2.67335 * U^2 + 73.7197 * U + 340.957 \quad (5b)$$

$$Q = -0.0008788 * U^4 + 0.096997 * U^3 - 3.97865 * U^2 + 97.3271 * U + 181.859 \quad (5c)$$

Congestion Regime

The congestion regime for each speed–flow curve was the same as Equation 2. It represented traffic conditions with heavy congestion. For each data set, the congestion regime represented the speed–flow relationship in the work zone when the flow rate fell below 1,300 pcphpl.

Final Form of the Four-Regime Speed–Flow Curves

After the upper and lower transition models were selected, four-regime models resulted for base, police, and SPE. They are summarized as follows:

For the base model:

- Q does not depend on speed, if $U = 61.3$;
- Q = Equation 4*a*, if $53.4 \le U < 61.3$;
- Q = Equation 5*a*, if $25.0 < U \le 53.4$; and
- Q = Equation 2, if $0 \le U < 25.0$.

For the police model:

- Q does not depend on speed, if $U = 55.0$;
- Q = Equation 4*b*, if $50.0 \le U < 55.0$;
- Q = Equation 5*b*, if $25.0 < U \le 50.0$; and
- Q = Equation 2, if $0 \le U < 25.0$.

For the SPE model:

- Q does not depend on speed, if $U = 54.5$;
- Q = Equation 4*c*, if $47.3 \le U < 54.5$;
- Q = Equation 5*c*, if $25.0 < U \le 47.3$; and
- Q = Equation 2, if $0 \le U < 25.0$.

Figure 4, *a*, *b*, and *c*, shows the four-regime speed–flow curves superimposed over the three-regime speed–flow curves for the base,

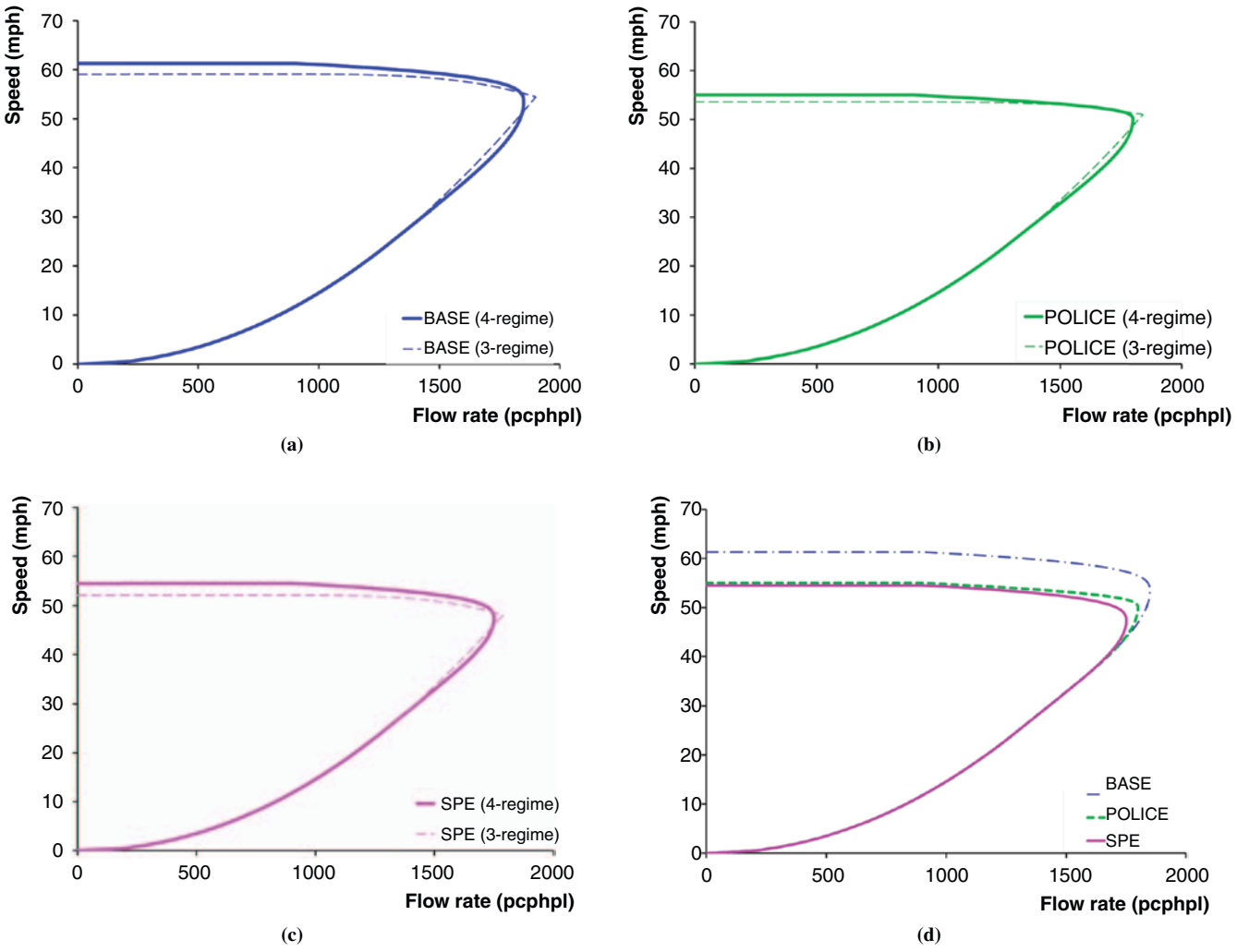

FIGURE 4 Four-regime speed–flow curves for (*a*) base, (*b*) police, and (*c*) SPE data and (*d*) for all three scenarios.

police, and SPE data, respectively. Figure 4*d* shows the four-regime speed–flow curves for all three cases on the same chart. As the figure shows, both the police and SPE implementation led to significant reductions in speed in the upper branch of the speed–flow curve. Because of those speed reductions, the work zone capacity was slightly reduced in both cases as compared with the base data.

Final Discussion

Three issues should be discussed. The first relates to the procedure to determine work zone capacity. It may be argued that work zone capacity should be equal to the volume given at the intersection of the upper transition model with the congested regime models in the three-regime model. The problems with the three-regime model have been discussed already, and are inherent when such models are used to find capacity. In fact, the actual work zone capacity that can be determined from the field data does not depend on the shape of the curve that is fitted for the rest of the data points. In the approach used here, work zone capacity was determined from the field data. Then the speed–flow curves were required to go through this important data point. This approach is proposed as better than to rely on the intersection of the two curves when field data are available. If field data are not available to find work zone capacity but other data points are available to fit a curve to the data point (an odd situation), then the intersection may be used to estimate work zone capacity.

The second issue relates to the goodness of fit of the upper transition regime models given in Equation 4, *a*, *b*, and *c*, to the field data. Because the fourth-degree spline equations were not built on the basis of the least-squares estimation, it may be argued that the spline equations are inferior to the regression equations in terms of goodness of fit. To investigate, the root mean square error in speed was computed for both the regression and the spline equations. For the base, police, and SPE data, the root mean square errors were 1.9, 1.4, and 1.7 mph from the regression Equation 1, *a*, *b*, and *c*, respectively; and 2.0, 1.6, and 1.9 mph from the spline Equations 4, *a*, *b*, and *c*, respectively. The root mean square errors given by the fourth-degree splines were comparable to those given by the regression equations. Thus it can be concluded that the goodness of fit of the spline equations to the data was not inferior but was almost as good as the regression equations.

One last issue concerns the duration of the three data sets. Each set included 1 h of traffic flow data, and the question is whether 1 h was sufficient to determine work zone capacity. An unused 1 h of SPE data was available to investigate. The 1-h data set was collected in the same work zone on I-55 during the SPE presence but not used to determine work zone speed–flow curves and capacity. The unused data set was analyzed with the methodology suggested by Ramezani et al. (*29*) to estimate work zone capacity during the SPE presence. The work zone capacity returned by the unused 1-h data set was close to the work zone capacity returned by the other 1 h of SPE data (Table 1). The work zone capacity was estimated as 1,759 pcphpl from the unused 1 h of SPE data. The work zone capacity of 1,759 pcphpl corresponded well with the 1,753 pcphpl returned by the other 1 h of SPE data. Thus the 1-h data set used to estimate work zone capacity was sufficient in this study. Of course it may be necessary to use data for a longer period of time if the data points are aggregated over longer time intervals (e.g., 15 min). In this study, speed and headway data were available for individual vehicles, and the data could be aggregated during any time interval. A 2-min time interval was used to aggregate data and provided 60 data points (over two lanes) for each data set, which was sufficient to build the models.

CONCLUSIONS AND RECOMMENDATIONS

- Four-regime speed–flow curves were developed through improvement of the three-regime speed–flow curves on the basis of the field data. Compared with the three-regime models, the four-regime models provided a more realistic picture of the speed–flow relationship of work zones in close-to-capacity conditions.
- A new method to find the optimal speed is proposed. The new method can be employed when a particular data set does not have enough data points at capacity conditions, which was the case in all three data sets in this study. In the new method, the regression curves of the three-regime models are used to estimate the optimal speed.
- The work zone capacity was estimated as 1,850 pcphpl for the base data (i.e., no speed-reduction treatment was present in the work zone other than the traditional signage cited in the *Manual on Uniform Traffic Control Devices*).
- Compared with the base scenario, police and SPE led to significant speed reductions in the upper (uncongested) branch of the speed–flow curve of the work zone. Compared with the base scenario, those speed reductions resulted in a slight capacity drop by about 50 and 100 pcphpl for the police and SPE scenarios, respectively.
- The results contributed to the accurate estimation of work zone capacity under different speed control treatments. Accurate estimation of work zone capacity enables more effective operation on a real-time basis and leads to more accurate diversion and traveler information for alternate routing and enhanced system reliability.
- It is recommended that this study be extended to consider work zones with different speed limits, lane configurations, and ITS.

REFERENCES

1. U.S. Department of Energy. *Temporary Losses of Highway Capacity and Impacts on Performance.* ORNL/TM-2002/3. Oak Ridge National Laboratory, Oak Ridge, Tenn., 2002.
2. *Snapshot of Peak Summer Work Zone Activity Reported on State Road Closure and Construction Websites.* FHWA, U.S. Department of Transportation, 2002.
3. National Work Zone Safety Information Clearinghouse. *Fatalities in Motor Vehicle Traffic Crashes by State and Work Zone.* Sept. 16, 2010. http://www.workzonesafety.org/crash_data/workzone_fatalities/2009. Accessed July 31, 2011.
4. Mohan, S. B., and P. Gautam. Cost of Highway Work Zone Injuries. *Practice Periodical on Structural Design and Construction,* Vol. 7, No. 2, 2002, pp. 68–73.
5. Garber, N. J., and M. Zhao. Distribution and Characteristics of Crashes at Different Work Zone Locations in Virginia. In *Transportation Research Record: Journal of the Transportation Research Board, No. 1794,* Transportation Research Board of the National Academies, Washington, D.C., 2002, pp. 19–28.
6. Salem, O. M., A. M. Genaidy, H. Wei, and N. Deshpande. Spatial Distribution and Characteristics of Accident Crashes at Work Zones of Interstate Freeways in Ohio. *Proc., ITSC 2006: 2006 IEEE Intelligent Transportation Systems Conference,* Toronto, Ontario, Canada, IEEE, New York, 2006, pp. 1642–1647.
7. Noel, E. C., C. L. Dudek, O. J. Pendleton, and Z. A. Sabra. Speed Control Through Freeway Work Zones: Techniques Evaluation. In *Transportation Research Record 1163,* TRB, National Research Council, Washington, D.C., 1988, pp. 31–42.
8. Zech, W. C., S. Mohan, and J. Dmochowski. Evaluation of Rumble Strips and Police Presence as Speed Control Measures in Highway

Work Zones. *Practice Periodical on Structural Design and Construction,* Vol. 10, No. 4, 2005, pp. 267–275.
9. Miller, L., F. Mannering, and D. M. Abraham. Effectiveness of Speed Control Measures on Nighttime Construction and Maintenance Projects. *Journal of Construction Engineering and Management,* Vol. 135, No. 7, 2009, pp. 614–619.
10. Chitturi, M., R. F. Benekohal, A. Hajbabaie, M.-H. Wang, and J. C. Medina. Effectiveness of Automated Speed Enforcement in Work Zones. *ITE Journal,* Vol. 80, No. 6, 2010, pp. 26–35.
11. Benekohal, R. F., M.-H. Wang, M. V. Chitturi, A. Hajbabaie, and J. C. Medina. Speed Photo-Radar Enforcement and Its Effects on Speed in Work Zones. In *Transportation Research Record: Journal of the Transportation Research Board, No. 2096,* Transportation Research Board of the National Academies, Washington, D.C., 2009, pp. 89–97.
12. Benekohal, R. F., M. V. Chitturi, A. Hajbabaie, M.-H. Wang, and J. C. Medina. Automated Speed Photo Enforcement Effects on Speeds in Work Zones. In *Transportation Research Record: Journal of the Transportation Research Board, No. 2055,* Transportation Research Board of the National Academies, Washington, D.C., 2008, pp. 11–20.
13. *Highway Capacity Manual.* TRB, National Research Council, Washington, D.C., 2000.
14. Benekohal, R. F., A.-Z. Kaja-Mohideen, and M. V. Chitturi. Methodology for Estimating Operating Speed and Capacity in Work Zones. In *Transportation Research Record: Journal of the Transportation Research Board, No. 1883,* Transportation Research Board of the National Academies, Washington, D.C., 2004, pp. 103–111.
15. Jiang, Y. Traffic Capacity, Speed, and Queue-Discharge Rate of Indiana's Four-Lane Freeway Work Zones. In *Transportation Research Record: Journal of the Transportation Research Board, No. 1657,* TRB, National Research Council, Washington, D.C., 1999, pp. 10–17.
16. Al-Kaisy, A., M. Zhou, and F. Hall. New Insights into Freeway Capacity at Work Zones: Empirical Case Study. In *Transportation Research Record: Journal of the Transportation Research Board, No. 1710,* TRB, National Research Council, Washington, D.C., 2000, pp. 154–160.
17. Dixon, K. K., J. E. Hummer, and A. R. Lorscheider. Capacity for North Carolina Freeway Work Zones. In *Transportation Research Record 1529,* TRB, National Research Council, Washington, D.C., 1996, pp. 27–34.
18. Maze, T., S. Schrock, and A. Kamyab. Capacity of Freeway Work Zone Lane Closures. *Mid-Continent Transportation Symposium Conference Proceedings,* University of Iowa, Ames, 2000, pp. 178–183.
19. Kim, T., D. J. Lovell, M. Hall, and J. Paracha. A New Methodology to Estimate Capacity for Freeway Work Zones. CD-ROM. Preprints of 80th Annual Meeting of the Transportation Research Board, Washington, D.C., 2001.
20. Karim, A., and H. Adeli. Radial Basis Function Neural Network for Work Zone Capacity and Queue Estimation. *Journal of Transportation Engineering,* Vol. 129, No. 5, 2003, pp. 494–503.
21. Adeli, H., and X. Jiang. Neuro-Fuzzy Logic Model for Freeway Work Zone Capacity Estimation. *Journal of Transportation Engineering,* Vol. 129, No. 5, 2003, pp. 484–493.
22. Benekohal, R. F., A.-Z. Kaja-Mohideen, and M. V. Chitturi. Methodology for Estimating Operating Speed and Capacity in Work Zones. In *Transportation Research Record: Journal of the Transportation Research Board, No. 1883,* Transportation Research Board of the National Academies, Washington, D.C., 2004, pp. 103–111.
23. Racha, S., M. Chowdhury, W. Sarasua, and Y. Ma. Analysis of Work Zone Traffic Behavior for Planning Applications. *Transportation Planning and Technology,* Vol. 31, No. 2, 2008, pp. 183–199.
24. Kang, K.-P., G.-L. Chang, and N. Zou. Optimal Dynamic Speed-Limit Control for Highway Work Zone Operations. In *Transportation Research Record: Journal of the Transportation Research Board, No. 1877,* Transportation Research Board of the National Academies, Washington, D.C., 2004, pp. 77–84.
25. Kang, K.-P., G.-L. Chang, and J. Panacha. Dynamic Late Merge Control at Highway Work Zones: Evaluations, Observations, and Suggestions. In *Transportation Research Record: Journal of the Transportation Research Board, No. 1948,* Transportation Research Board of the National Academies, Washington, D.C., 2006, pp. 86–95.
26. Yulong, P., and D. Leilei. Study on Intelligent Lane Merge Control System for Freeway Work Zones. *Proc., 10th International IEEE Conference on Intelligent Transportation Systems,* Seattle, Wash., IEEE, New York, 2007, pp. 586–591.
27. Avrenli, K. A., R. F. Benekohal, and H. Ramezani. Determining Speed-Flow Relationship and Capacity for Freeway Work Zone with No Lane Closure. Presented at 90th Annual Meeting of the Transportation Research Board, Washington, D.C., 2011.
28. Avrenli, K. A., R. Benekohal, and H. Ramezani. Traffic Flow Characteristics and Capacity in Police-Enforced and Intelligent Work Zones. *Procedia—Social and Behavioral Sciences,* Vol. 16, Elsevier, Amsterdam, Netherlands, 2011.
29. Ramezani, H., R. F. Benekohal, and K. A. Avrenli. Methodology to Measure Work Zone Capacity Using Field Data. Presented at 90th Annual Meeting of the Transportation Research Board, Washington, D.C., 2011.

The Work Zone Traffic Control Committee peer-reviewed this paper.